Crystal structure and centromere binding of the plasmid segregation protein ParB from pCXC100

Lin Huang, Ping Yin, Xing Zhu, Yi Zhang and Keqiong Ye

Supplementary Materials (3 figures and 2 tables)

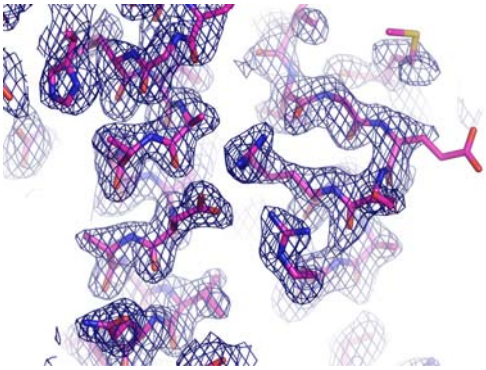

Figure S1. The experimental electron density map resulted from SIRAS phasing, phase extension and solvent modification. The map calculated to 1.9 Å resolution is contoured at 1σ and superimposed on the refined structure of the ParB RHH domain.

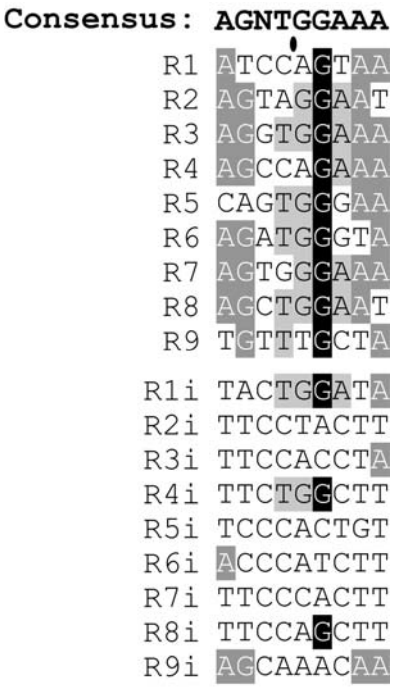

Figure S2. The centromere core is composed of 9 direct repeats. Repeats R1-R9 and their reverse and complementary sequences R1i-R9i (inverted repeats) are lined up by the ParB binding centers (ellipse). Nucleotides that occur in at least 100%, 75% and 50% direct repeats are shaded in black, gray and light gray, respectively. Nucleotides in inverted repeats conforming to the consensus sequence are shaded similarly as in direct repeats. None of inverted repeats are aligned to the consensus sequence better than their direct counterparts. Only R1 seems to align equally well in either directions.

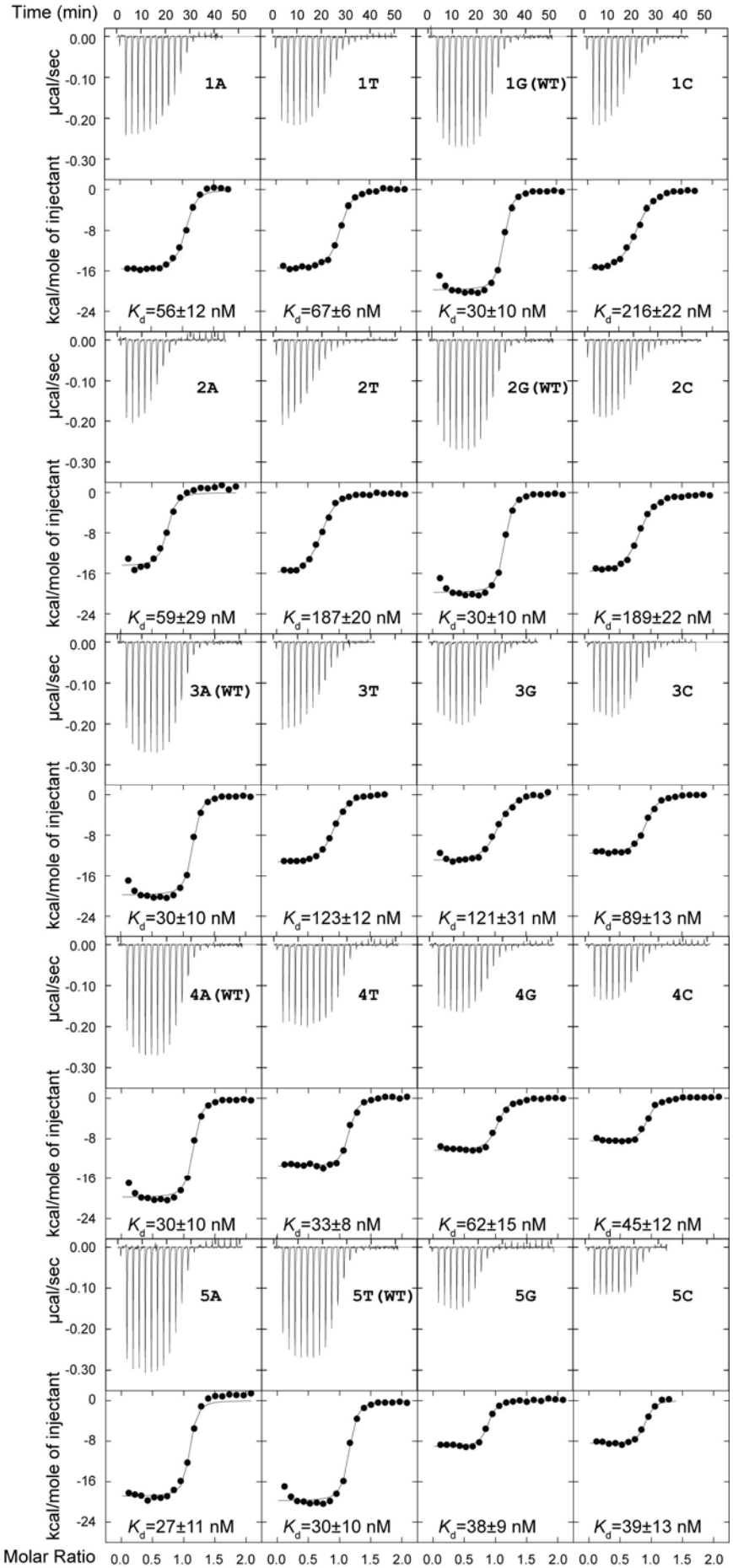
Time (min)
0 10 20 30 40 50
µcal/sec
0.00
-0.10
-0.20
-0.30
kcal/mole of injectant
0
-8
-16
-24
1A
1T
1G (WT)
1C
Kd=56±12 nM
Kd=67±6 nM
Kd=30±10 nM
Kd=216±22 nM
2A
2T
2G (WT)
2C
Kd=59±29 nM
Kd=187±20 nM
Kd=30±10 nM
Kd=189±22 nM
3A (WT)
3T
3G
3C
Kd=30±10 nM
Kd=123±12 nM
Kd=121±31 nM
Kd=89±13 nM
4A (WT)
4T
4G
4C
Kd=30±10 nM
Kd=33±8 nM
Kd=62±15 nM
Kd=45±12 nM
5A
5T (WT)
5G
5C
Kd=27±11 nM
Kd=30±10 nM
Kd=38±9 nM
Kd=39±13 nM
Molar Ratio
0.0 0.5 1.0 1.5 2.0

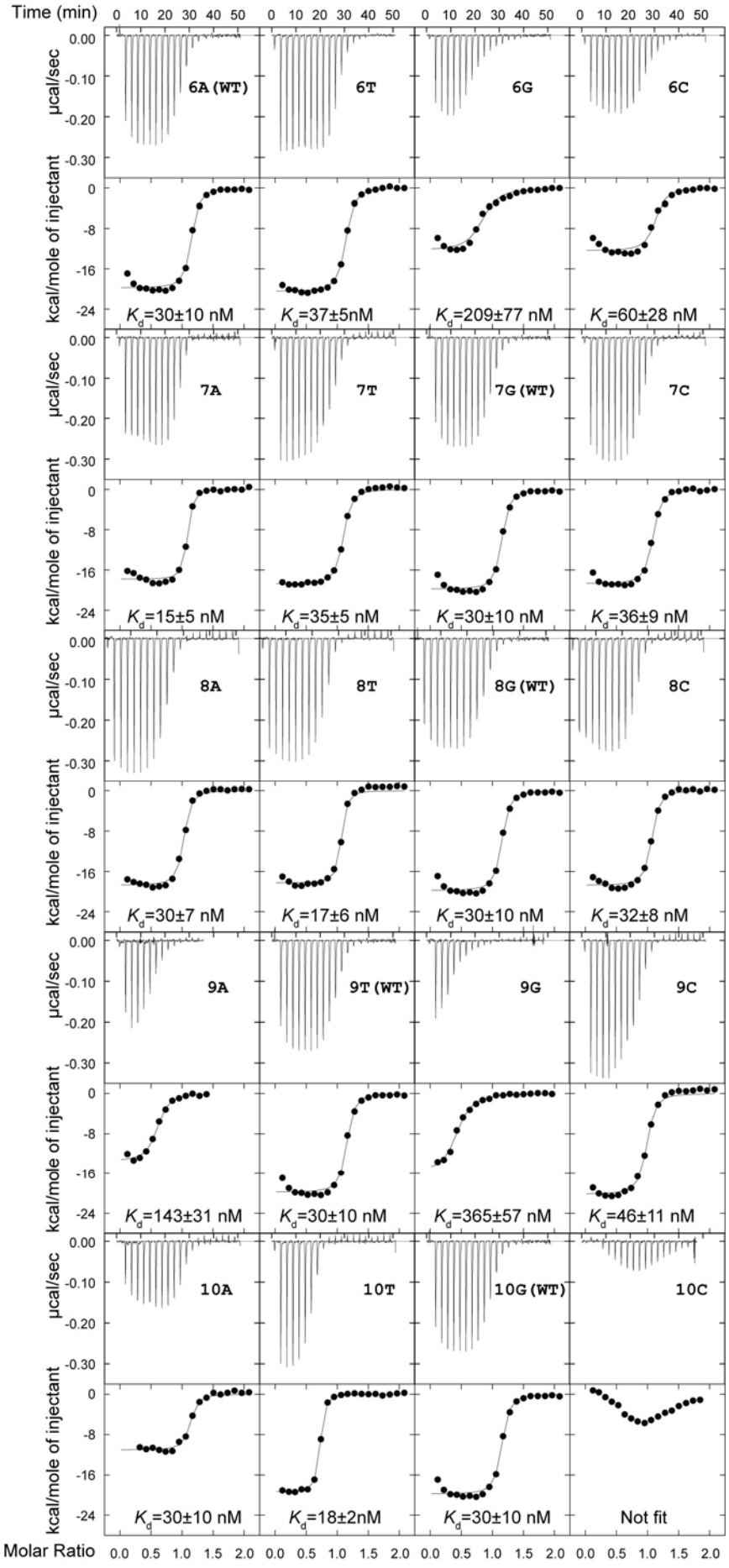
Time (min)
0 10 20 30 40 50
µcal/sec
0.00
-0.10
-0.20
-0.30
kcal/mole of injectant
0
-8
-16
-24
6A (WT)
K_d=30±10 nM
6T
K_d=37±5nM
6G
K_d=209±77 nM
6C
K_d=60±28 nM
7A
K_d=15±5 nM
7T
K_d=35±5 nM
7G (WT)
K_d=30±10 nM
7C
K_d=36±9 nM
8A
K_d=30±7 nM
8T
K_d=17±6 nM
8G (WT)
K_d=30±10 nM
8C
K_d=32±8 nM
9A
K_d=143±31 nM
9T (WT)
K_d=30±10 nM
9G
K_d=365±57 nM
9C
K_d=46±11 nM
10A
K_d=30±10 nM
10T
K_d=18±2nM
10G (WT)
K_d=30±10 nM
10C
Not fit
Molar Ratio
0.0 0.5 1.0 1.5 2.0

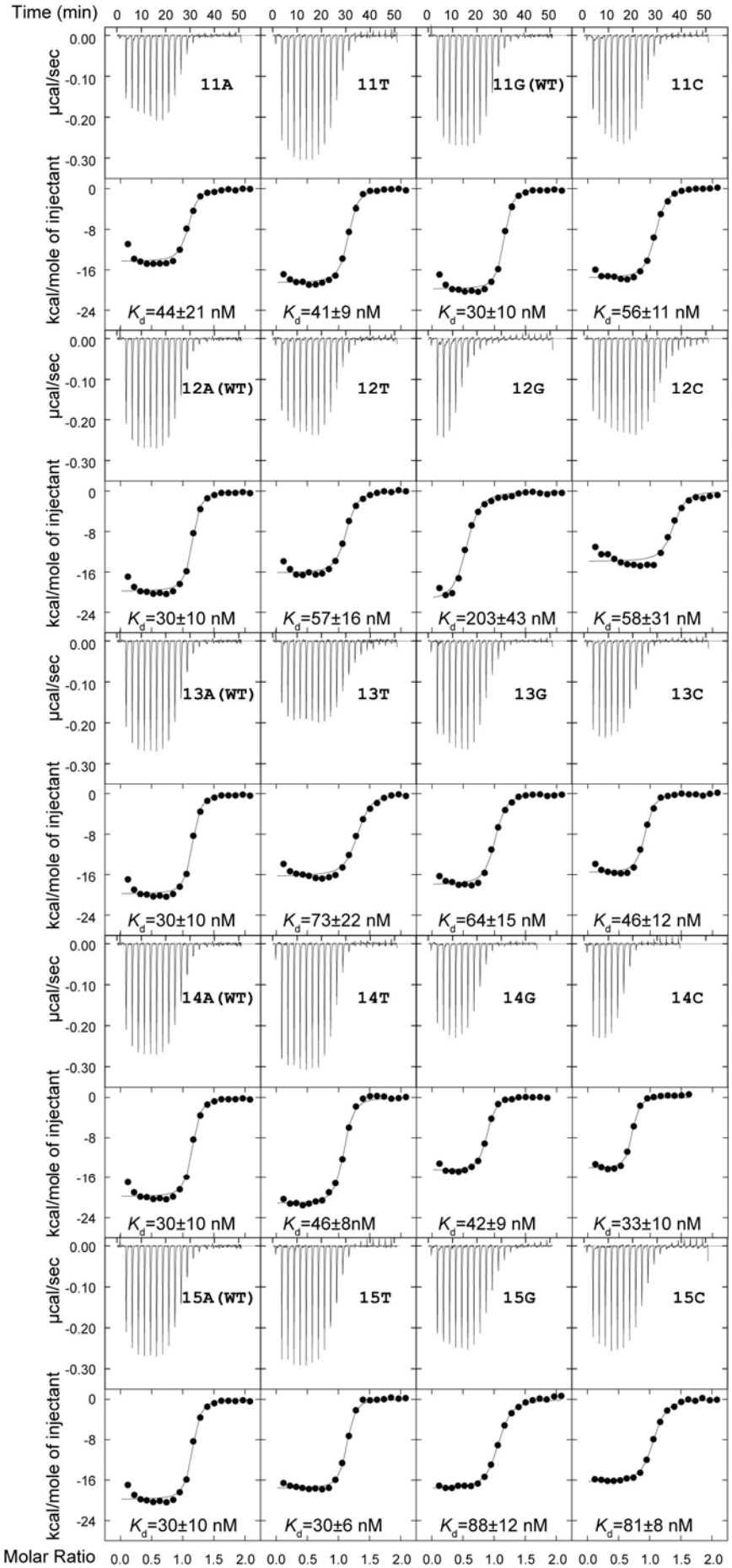
Time (min)
0 10 20 30 40 50
µcal/sec
0.00
-0.10
-0.20
-0.30
kcal/mole of injectant
0
-8
-16
-24
11A
11T
11G (WT)
11C
Kd=44±21 nM
Kd=41±9 nM
Kd=30±10 nM
Kd=56±11 nM
12A (WT)
12T
12G
12C
Kd=30±10 nM
Kd=57±16 nM
Kd=203±43 nM
Kd=58±31 nM
13A (WT)
13T
13G
13C
Kd=30±10 nM
Kd=73±22 nM
Kd=64±15 nM
Kd=46±12 nM
14A (WT)
14T
14G
14C
Kd=30±10 nM
Kd=46±8nM
Kd=42±9 nM
Kd=33±10 nM
15A (WT)
15T
15G
15C
Kd=30±10 nM
Kd=30±6 nM
Kd=88±12 nM
Kd=81±8 nM
Molar Ratio
0.0 0.5 1.0 1.5 2.0

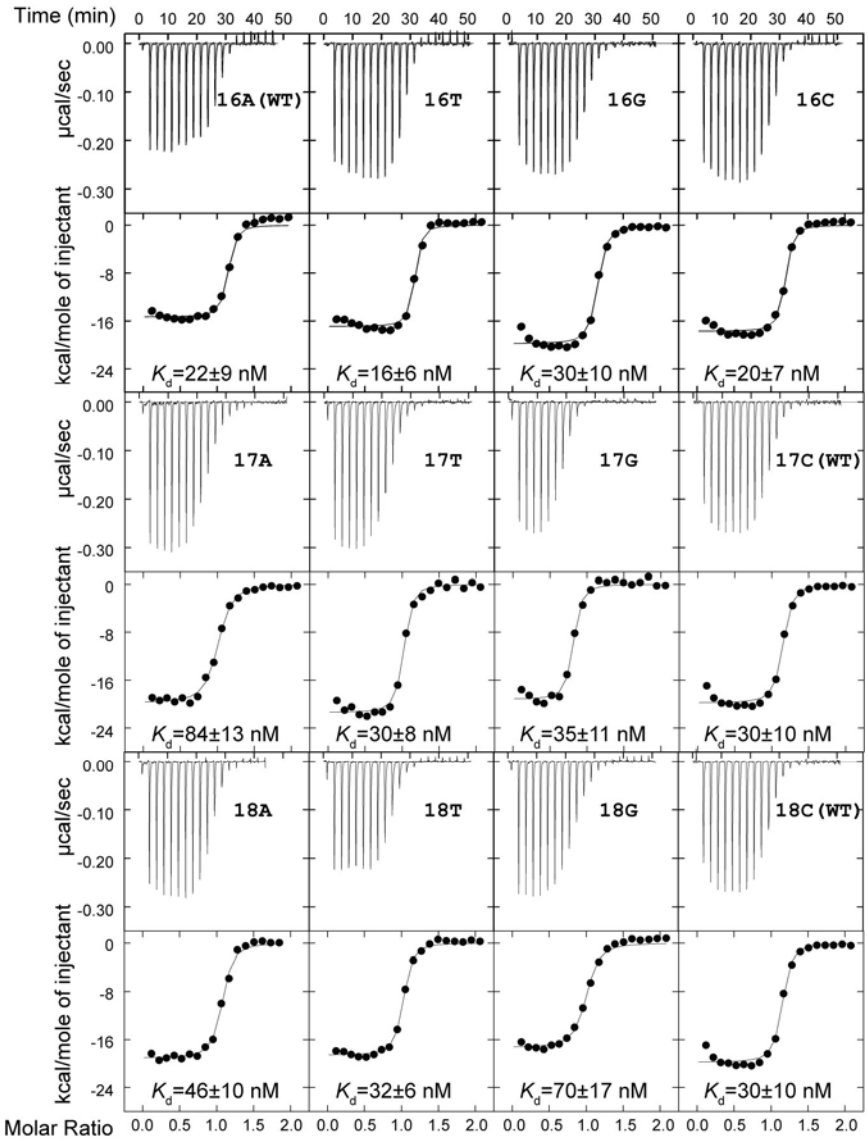

Figure S3. ITC profiles of R3-18 point mutants. Wild type R3-18 was shown in each row for comparison. The curves are the best fit to a one-set-of-sites model.

Table S1. Sequence of the forward strand of double-stranded DNA probes used in this study

Probe	Sequence (5'-3')
R3-14	AATAGGTGGAAAAG
R3-16	GAATAGGTGGAAAAGC
R3-20	AGGAATAGGTGGAAAAGCCA
R3-22	TAGGAATAGGTGGAAAAGCCAG
R4-14	AAAAGCCAGAAACA
R4-16	GAAAAGCCAGAAACAG
R4-20	TGGAAAAGCCAGAAACAGTG
R0-18	TGCTCGATCTGGCTATCC
R1-18	TGGCTATCCAGTAAAGTA
R2-18	AGTAAAGTAGGAATAGGT
R3-18	GGAATAGGTGGAAAAGCC
R4-18	GGAAAAGCCAGAAACAGT
R5-18	AGAAACAGTGGGAAAGAT
R6-18	GGGAAAGATGGGTAAGTG
R7-18	GGGTAAGTGGGAAAAGCT
R8-18	GGAAAAGCTGGAATTGTT
R9-18	GGAATTGTTTGCTACGGT
R10-18	TGCTACGGTAGAACACGC
R11-18	AGAACACGCCGAACGGCC
R4-18-3	GGTGGAAAAGCCAGAAAC
R4-18-2	GTGGAAAAGCCAGAAACA
R4-18-1	TGGAAAAGCCAGAAACAG
R4-18+1	GAAAAGCCAGAAACAGTG
R4-18+2	AAAAGCCAGAAACAGTGG
R4-18+3	AAAGCCAGAAACAGTGGG
R4-18+4	AAGCCAGAAACAGTGGGA
R2R3-18	AGTAGGAATAGGTGGAAA
R2R3-27	AGTAAAGTAGGAATAGGTGGAAAAGCC
1R3'-18	GGAAAAGGTGGAAAAGGT
2R3'-27	GGAAAAGGTGGAAAAGGTGGAAAAGGT
1R6'-18	GGGTAAGATGGGTAAGAT
2R6'-27	GGGTAAGATGGGTAAGATGGGTAAGAT

Table S2. Thermodynamic parameters of binding of ParB 65-139 to the centromere DNA as determined using ITC.

Probe	*n*	*K*	K_d	Δ*H*	Δ*S*
		10^6 M^{-1}	nM	kcal mol^{-1}	kcal mol^{-1} K^{-1}
R1-18	1.4±0.1	1.1±0.7	950±680	-8±1	1.27
R2-18	1.0±0.1	2.7±0.7	380±100	-14±1	-18.3
R3-18	1.0±0.1	32±12	31±12	-18±1	-25.7
R4-18	0.9±0.1	12±8	87±59	-12±1	-6.7
R5-18	1.4±0.1	1.3±0.5	780±320	-7±1	-4.7
R6-18	1.2±0.2	1.4±1	700±470	-11±2	-8.0
R7-18	Not fit				
R8-18	1.1±0.1	18±4	56±12	-22±1	-39.4
R9-18	0.8±0.1	90±71	11±9	-17±1	-20.2
R3-14	0.7±0.1	0.23±0.07	4300±1300	-10±1	-9.1
R3-16	0.6±0.1	2.0±0.3	510±90	-20±1	-38.5
R3-18	1.0±0.1	27±7	37±10	-19±1	-30.6
R4-14	No binding				
R4-16	0.7±0.1	1.9±0.2	530±50	-8±1	2.0
R4-18	0.9±0.1	17±3	60±12	-13±1	-10.9
R4-20	1.2±0.1	15±10	68±48	-9±1	4.2
R3-18	1.1±0.1	33±11	30±10	-20±1	-32.0
R3-18-1A	1.0±0.1	18±4	56±12	-16±1	-19.5
R3-18-1T	1.0±0.1	15±1	67±6	-16±1	-19.3
R3-18-1C	0.8±0.1	5±1	216±22	-16±1	-22.8
R3-18-2A	0.7±0.1	17±8	59±29	-15±1	-15.6
R3-18-2T	0.7±0.1	5±1	187±20	-16±1	-23.3
R3-18-2C	0.8±0.1	5±1	189±22	-16±1	-22.8
R3-18-3T	0.9±0.1	8±1	123±12	-13±1	-13.5
R3-18-3G	1.0±0.1	8±2	121±31	-13±1	-12.1
R3-18-3C	0.9±0.1	11±2	89±13	-12±1	-7.6
R3-18-4T	1.1±0.1	30±7	33±8	-13±1	-10.9
R3-18-4G	1.0±0.1	16±4	62±15	-10±1	-1.62
R3-18-4C	0.9±0.1	22±6	45±12	-8±1	5.28
R3-18-5A	1.1±0.1	37±15	27±11	-19±1	-28.9
R3-18-5G	0.8±0.1	26±6	38±9	-9±1	3.59
R3-18-5C	0.9±0.1	25±9	39±13	-8±1	5.56
R3-18-6T	1.1±0.1	27±4	37±5	-21±1	-34.7
R3-18-6G	0.8±0.1	5±2	209±77	-12±1	-10.9
R3-18-6C	1.1±0.1	17±8	60±28	-12±1	-8.59
R3-18-7A	1.0±0.1	66±24	15±5	-18±1	-24.0
R3-18-7T	1.1±0.1	29±4	35±5	-19±1	-28.9

R3-18-7C	1.0±0.1	28±7	36±9	-19±1	-28.7
R3-18-8A	1.0±0.1	33±8	30±7	-19±1	-28.4
R3-18-8T	1.0±0.1	58±21	17±6	-18±1	-25.8
R3-18-8C	1.0±0.1	32±8	32±8	-19±1	-28.6
R3-18-9A	0.6±0.1	7±2	143±31	-13±1	-13.7
R3-18-9G	0.4±0.1	3±0.4	365±57	-16±1	-23.7
R3-18-9C	0.9±0.1	22±6	46±11	-20±1	-34.1
R3-18-10A	1.1±0.1	33±11	30±10	-11±1	-2.61
R3-18-10T	0.7±0.1	54±6	18±2	-19±1	-28.5
R3-18-10C	Not fit				
R3-18-11A	1.1±0.1	23±11	44±21	-14±1	-14.3
R3-18-11T	1.1±0.1	24±5	41±9	-19±1	-28.5
R3-18-11C	1.0±0.1	18±4	56±11	-18±1	-26
R3-18-12T	1.1±0.1	17±5	57±16	-16±1	-21.3
R3-18-12G	0.5±0.1	5±1	203±43	-22±1	-42.8
R3-18-12C	1.3±0.1	17±9	58±31	-14±1	-13.5
R3-18-13T	1.3±0.1	14±4	73±22	-16±1	-22.0
R3-18-13G	1.0±0.1	16±4	64±15	-18±1	-27.4
R3-18-13C	0.9±0.1	22±6	46±12	-16±1	-18.6
R3-18-14T	1.0±0.1	22±4	46±8	-21±1	-37.5
R3-18-14G	0.8±0.1	24±5	42±9	-14±1	-14.6
R3-18-14C	0.7±0.1	30±9	33±10	-14±1	-12.6
R3-18-15T	1.1±0.1	33±7	30±6	-18±1	-24.6
R3-18-15G	1.0±0.1	11±2	88±12	-18±1	-27.1
R3-18-15C	1.0±0.1	12±1	81±8	-16±1	-22.4
R3-18-16A	1.1±0.1	46±20	22±9	-15±1	-16.4
R3-18-16T	1.2±0.1	64±24	16±6	-17±1	-21.0
R3-18-16C	1.2±0.1	50±17	20±7	-18±1	-24.2
R3-18-17A	1.0±0.1	12±2	84±13	-20±1	-34.1
R3-18-17T	1.0±0.1	34±10	30±8	-21±1	-37.4
R3-18-17G	0.8±0.1	29±9	35±11	-19±1	-30.3
R3-18-18A	1.0±0.1	22±5	46±10	-19±1	-30.5
R3-18-18T	1.0±0.1	31±6	32±6	-19±1	-28.1
R3-18-18G	1.0±0.1	14±3	70±17	-17±1	-25.4
R3-18	1.0±0.1	34±14	29±12	-18±1	-24.9
R9-18	0.9±0.1	59±21	17±6	-21±1	-33.9

The first 9 ITC experiments were preformed by titrating 50 μM dimeric ParB 65-139 into 5 μM DNA, and the remaining experiments were preformed by titrating 100 μM dimeric ParB 65-139 into 10 μM DNA.

To ensure the consistence of experiment, some titrations, for example R3-18, were preformed multiple times with different machines, batches of DNA and experimental settings.

The parameters were derived from fitting of ITC data to a one-set-of-sites model. Errors from fitting are reported.